Research Article

Long-term administration of red ginseng non-saponin fraction rescues the loss of skeletal muscle mass and strength associated with aging in mice

Da-Eun Cho [a], Gwang-Muk Choi [a], Yong-Seok Lee [a], Joon-Pyo Hong [a], Mijung Yeom [b], Bombi Lee [b], Dae-Hyun Hahm [a, b, c, d, *]

[a] *Department of Biomedical Sciences, Graduate School, Kyung Hee University, Seoul, Republic of Korea*
[b] *Acupuncture and Meridian Science Research Center, Kyung Hee University, Seoul, Republic of Korea*
[c] *Department of Physiology, College of Medicine, Kyung Hee University, Seoul, Republic of Korea*
[d] *BioNanocomposite Research Center, Kyung Hee University, Seoul, Republic of Korea*

A R T I C L E   I N F O

A B S T R A C T

Background: Sarcopenia is a new and emerging risk factor aggravating the quality of life of elderly population. Because Korean Red Ginseng (RG) is known to have a great effect on relieving fatigue and enhancing physical performance, it is invaluable to examine its potential as an anti-sarcopenic drug.
Methods: Anti-sarcopenic effect of non-saponin fraction of Korean Red Ginseng (RGNS) was evaluated in C2C12 myoblasts treated with C2-ceramide to induce senescence phenotypes, and 22-month-old mice fed with chow diet containing 2% RGNS (w/w) for 4 further months.
Results: The RGNS treatment significantly alleviated cellular senescence indicated by intracellular lipid accumulation, increased amount of lysosomal β-galactosidase, and reduced proliferative capacity in C2C12 myoblasts. This effect was not observed with saponin fraction. In an aged mouse, the 4-month-RGNS diet significantly improved aging-associated loss of muscle mass and strength, assessed by the weights of hindlimb skeletal muscles such as tibialis anterior (TA), extensor digitorum longus (EDL), gastrocnemius (GN) and soleus (SOL), and the cross-sectional area (CSA) of SOL muscle, and the behaviors in grip strength and hanging wire tests, respectively. During the same period, an aging-associated shift of fast-to slow-twitch muscle in SOL muscle was also retarded by the RGNS treatment.
Conclusions: These findings suggested that the long-term diet of RGNS significantly prevented aging-associated muscle atrophy and reduced physical performance, and thus RGNS has a strong potential to be developed as a drug that prevents or improves sarcopenia.
© 2021 The Korean Society of Ginseng. Publishing services by Elsevier B.V. This is an open access article under the CC BY-NC-ND license (http://creativecommons.org/licenses/by-nc-nd/4.0/).

1. Introduction

Despite the increase in life expectancy over the last 200 years, aging-related illnesses such as cancer and cardiovascular, neuro-degenerative and metabolic diseases are emerging as a new risk factor in the developed countries [1,2]. Besides these serious conditions, a senile dysfunction that has not been noticed so far is the loss of skeletal muscle mass and function in the elderly, termed "sarcopenia" [3–5]. Nowadays, sarcopenia is a primary risk factor for fall, bone fracture, frailty and physical disability of elderly population, which eventually leads to their poor quality of life and even mortality [6]. In principle, sarcopenia is caused by an imbalance between protein synthesis and autophagic degradation in the skeletal muscle cells [7], which is closely associated with hormone

balance, low-level inflammation, ectopic fat deposition, functionality of myosatellite cells [8–10]. As aging progresses, the differentiation capacity of myosatellite cells is gradually reduced and thus muscle mass and tone cannot be maintained [11]. Despite the clinical significance of aging-related sarcopenia, its underlying mechanism and pathophysiology has not been clearly resolved yet. Moreover, to date, there have been no effective therapies or US FDA-approved drugs for the treatment of sarcopenia except resistance exercise and nutrition although a lot of efforts have been done for the last decade [12].

In the Korean traditional medicine, red ginseng (RG) has been widely used to restore the homeostasis, boost vital energy, alleviate fatigue and improve blood flow as an adaptogenic herb [13,14]. For dozens of years, many researches have studied a variety of medicinal effects of RG such as anti-aging, anti-frailty and anti-cancer, and its underlying mechanisms [15–18]. Most studies have focused on the saponin fraction of RG that is prepared from butanol extraction [16–18]. In recent years, increasing attention has been paid to the non-saponin (NS) fraction of RG including polyacetylene- and phenol-based compounds in terms of their anticancer and anti-aging effects, respectively [19,20]. However, there has been little studies on the biological effects of NS fraction of RG, especially on aging-related sarcopenia. In the present study, antisarcopenic effect of NS fraction of RG was investigated in the in vitro senescence model of C2C12 myoblasts and the aged mouse model. The senescence phenotype of C2C12 myoblasts was manufactured by forceful accumulation of C2-ceramide into C2C12 myoblasts [21,22]. For in vivo evaluation of NS, aged mice were daily fed reformulated diet containing NS fraction of RG for 4 months and the alterations of their muscle strength and mass were analyzed.

2. Materials and methods

2.1. Saponin and non-saponin fractions of red ginseng

Saponin and non-saponin fractions of Korean Red Ginseng (RG) extracts were kindly provided by Korean Tobacco and Ginseng Company (Daejeon, Republic of Korea). Concentrated RG extract (2 kg) was prepared by stewing raw RG (4 kg) with distilled water, and freeze-dried to obtain the powder form (1.32 kg). The powder extract was dissolved in distilled water and transferred into a separating funnel and fractionated with equal volume of petroleum ether. The water fraction was successively fractionated with equal volume of water-saturated n-butanol three-times and then butanol fraction was fractionated with equal volume of distilled water again. Finally, the butanol (saponin fraction, RGS) and water (non-saponin, RGNS) fractions were freeze-dried using a lyophilizer. The crude saponin (130 g, 10.57% yield) and non-saponin (1100 g, 89.4% yield) powders were stored at −20 °C for future experiments.

3. In vitro study

3.1. Cell culture

A mouse skeletal muscle cell line (C2C12) was obtained from Korean Cell Line Bank (Jongno-gu, Seoul, South Korea). Cells were cultivated in the growth medium consisting of Dulbecco's Modified Eagles's Media (WELGENE, Gyeongsan-si, Gyeongsangbuk-do, South Korea) supplemented with 10% fetal bovine serum (WELGENE) and 1% penicillin/streptomycin (WELGENE) at 37 °C in a humidified incubator under 5% CO_2. In order to introduce senescence phenotypes, the cells were treated with 50 μM C2-ceramide (Sigma-Aldrich Chemical Co., St. Louis, MO, USA) for 8 h, 1 h earlier

before the RG(N)S treatment, according to the protocol of Jadhav et al. [21].

3.2. Intracellular lipid staining

Following the treatment period, the cells were washed and fixed in 10% formalin. The cells were then washed in 60% isopropyl alcohol for 10 min, dried, then stained in 2% (w/v) oil red O for 1 h at room temperature. Stained cells were visualized under a light microscope at both 10x and 40× magnification and the images were captured.

3.3. β-galactosidase assay

Following the treatment period, the cells were stained using the senescence β-galactosidase (β-gal) staining kit (Cell Signaling Technology Inc., Danvers, MA, USA). Briefly, following the treatment period, the cells were washed, fixed and stained β-gal staining solution. The incubated overnight at 37 °C. The cells were examined under an optical microscope (BX53, Olympus Co., Japan) at 40× magnification for detecting X-gal stain (blue). Images were captured with a camera for analysis of the percentage of stained versus non-stained cells.

3.4. Cell viability

Cell viability was assessed using the EZ-Cytox® assay kit (DoGen BIO, Guro-gu, Seoul, Korea) and trypan blue exclusion assay (Gibco, Life Technologies Corporation, Grand Island, NY, USA). Briefly, 10 μl EZ-Cytox® reagent was added to each well of 6-well plates. After incubating for 2 h at 37 °C, the plates were read at 450 nm using a microplate reader (VersaMax™ Tunable; Molecular Devices, Sunnyvale, CA, USA). For trypan blue assay, the cells were washed and then either immediately processed (0-h post) or the media was replaced with growth medium and allowed to grow for an additional 72 h (72-h post). Cells were collected in equal volume of growth medium, centrifuged, and resuspended in 200 μl of the medium. Resuspended cells were gently mixed with equal volume of 0.4% trypan blue (Gibco) and allowed to rest for 2 min. After that, 10 μl of the cells were loaded onto the hemocytometer, and total (blue and non-blue) and dead (blue) cells were counted. Cell concentration was calculated considering dilution factor.

3.5. BrdU cell proliferation assay

An ELISA-based assay kit (Cell Signaling Technology Inc.) for 5-bromo-2′-deocyuridine (BrdU) incorporation into DNA was used to determine cell proliferation. Briefly, after the drug treatments, the cells were pulsed with BrdU followed by adding fixing & denaturing solution and keeping the plate at room temperature for 30 min, incubated with a primary antibody against BrdU, and then incubated with a secondary-conjugated HRP-linked antibody. Finally, 3,30,5,500-tetramethylbenzidine as a substrate is added to the well resulting in a colorimetric change. After adding the stop solution, absorbance was read at 450 nm using a microplate reader (Molecular Devices).

3.6. Reverse transcriptase-polymerase chain reaction (RT-PCR)

Total RNA was extracted from C2C12 myoblasts using the TRIzol® reagent (Ambion, Thermo Fisher Scientific, Rockford, IL, USA) according to the manufacturer's protocol. The cDNA synthesis for mRNA was performed using PrimeScript™ RT Master Mix (TaKaRa Bio Co., Kusatsu, Japan). Quantitative real-time PCR was performed with the LightCycler® (Roche Molecular Systems, Inc., Basel,

Switzerland) using SYBR Green Mater Mix. The primer sequences and annealing temperatures used were as follows: atrogin-1: *F* 5′-TGTGGGTGTATCGGATGGAG-3′, *R* 5′-GGCAGAGTCTCTTCCACGT-3′ (62 °C); muscle RING-Finger Protein-1 (MuRF-1): *F* 5′-CAACCTGTGCCGCAAGTG-3′, *R* 5′-CAACCTCGTGCCTACAAGATG-3′ (62 °C), p21: *F* 5′-TCAGAGCCACAGGCACCAT-3′, *R* 5′-TCCACGG-GACCGAAGAGA-3′ (60 °C), p57: *F* 5′-TCTCTCGGGGATTCCAGGAC-3′, *R* 5′-CTTGCGCTTGGCGAAGAA-3′ (60 °C), pax7: *F* 5′-TAAGAGAGA-GAACCCCGGCA-3′, *R* 5′-GATGCCATCGATGCTGTGTT-3′ (58 °C), GAPDH: *F* 5′-AACGACCCCTTCATTGACCT-3′, *R* 5′-ATGT-TAGTGGGGTCTCGGTC-3′ (58 °C).

4. In vivo study

4.1. Animals and groups

Aged female C57BL/6 mice were obtained from Korea Basic Science Institute (KBSI, Gwangju, South Korea). The animal experiments were conducted in accordance with the Guide for the Care and use of Laboratory Animals (NIH Publications No. 80–23, revised in 1996) and approved by the Kyung Hee University Institutional Animal Care and Use Committee (KHUASP (SE)-19-051). The animals were maintained under environmentally controlled conditions (temperature: 22 ± 2 °C; humidity: 55 ± 16%) and a 12/12 h light/dark cycle (lights on at 08:00, lights off at 20:00) and were acclimated to these conditions before the experiment with free access to food and water for at least 1 week. The mice were divided randomly into three groups: 22-month-old mice fed a standard chaw (22CO, n = 8); 26-month-old mice fed a standard chaw (26CO, n = 8), 26-month-old mice fed the RGNS-containing diet for 4 months (26NS, n = 8). Experimental schedule is shown in Fig. 1. Reformulated diet containing 0.08% RGNS fraction (800 mg RGNS/kg-chaw) was manufactured by TodoBio (Gyeonggi-do, South Korea).

4.2. Grip strength test

A grip strength meter (FGP-5; Shimpo, Kyoto, Japan) was used to measure fore and hindlimb grip strength in parallel. The animals grasp a mesh grid with their four feet and the holding strength is delivered to the force meter. Peak values were recorded as maximum instantaneous readings captured by the meter during the course of a single pull of animal's tail. The values are expressed in unit of force (N) on a digital display unit. The mouse is given three trials per session with 30-s recovery interval.

4.3. Hanging wire test

Wire grip test was performed to accesses whole body force once a week for 4 months. A plastic-coated wire is secured to two vertical stands and maintained 35 cm above a thick layer of soft bedding to prevent animal injury when it falls down. When the mouse grips the middle of the wire with its fore limbs, a timer is stated. The time until the mouse completely releases its grasp and falls down is recorded. The mouse is given three trials per session with 30-s recovery interval.

4.4. Sectioning of skeletal muscles and hematoxylin and eosin-staining

Skeletal muscles in hindlimb such as TA, EDL, GN and SOL were dissected and their weights were measured using a digital balance (Mettler-Toledo Inc., Columbus, OH, USA). Of these muscles, SOL muscle was embedded in FSC 22 Clear frozen section compound (Leica Biosystems Richmond Inc., Richmond, IL, USA), frozen in liquid nitrogen-cooled isopentane and stored at −80 °C for further experiments. Each muscle was cut into 8 μm serial horizontal sections with a cryostat maintained at −20 °C. A portion of the entire circumference around the mid-belly was used. The sections were stained with hematoxylin (YD diagnostics Co., Youngin-si, South Korea) and eosin (Sigma-Aldrich Chemical Co.). All sections were observed and photographed under a microscope (BX53; Olympus Co.). The average muscle fiber size was quantified by measuring the cross-sectional area (CSA) of at least 100 randomly selected fibers from at least 3 sections of each muscle. The border of each fiber was manually demarcated using a calibrated pen, and then the area (μm^2) was automatically calculated using an Image J® software.
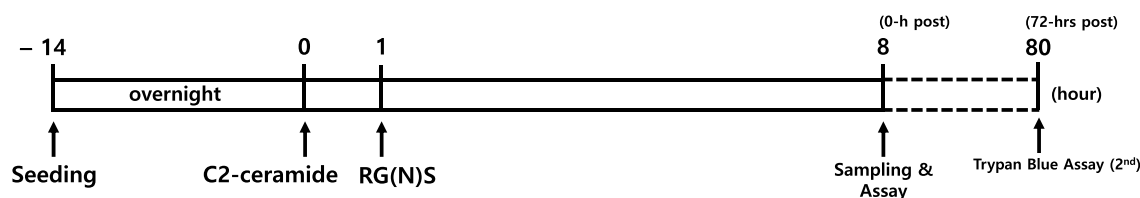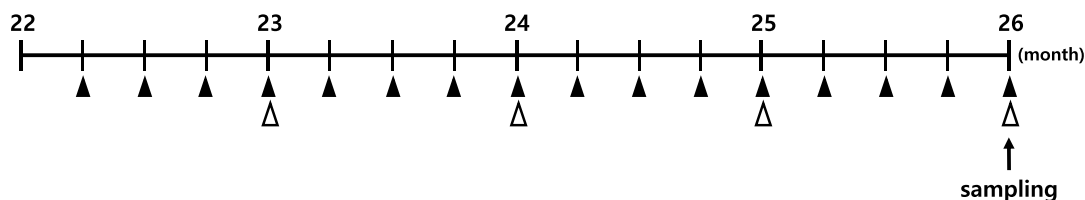
Fig. 1. Schematic diagrams illustrating in vitro (A) and in vivo (B) experimental schedules. In the in vitro study, 50 μM C2-ceramide was added to induce cell senescence on hour 1, and the drugs such as RGS or RGNS were treated 1 h earlier. In the in vivo study, body weight and food intake were measured once a week (closed triangle) and behavior tests were once a month (open triangle). RGNS: non-saponin fraction of red ginseng.

4.5. Immunofluorescent staining for muscle fiber type classification

At least 3 sections per each mouse were selected for immunofluorescence staining. The selected sections were air-dried (entire procedure performed at room temperature) for 10 min and incubated with 1% Triton X-100 for 30 min. The sections were blocked in 10% goat serum in PBS for 2 h. Anti-mouse MHC I (BA-F8), IIa (SC-71) and IIb (BF−F3) bovine primary antibodies were purchased from the Developmental Studies Hybridoma Bank in University of Iowa (Iowa City, IA, USA). The sections were stored in primary antibody cocktail solution at 4 °C for overnight. After washing with 0.1% Tween 20 for 5 min, 3 times, the sections were incubated in anti-bovine secondary antibodies conjugated to fluorescence dyes such as Alexa Fluor™ 647, 488 and 555 (Molecular Probes of Thermo Fisher Scientific, Rockford, IL, USA) for 2 h. Finally, the sections were mounted coverslips with VAECTASHIELD® Mounting Medium. The samples were examined with a confocal laser scanning microscope (Fluoview FV10i; Olympus Co., Japan).

4.6. Statistical analysis

All of the measurements were performed by an independent investigator blind to the experimental conditions, and the results are expressed as mean ± standard error of the mean (SEM). Differences within or between normally distributed data were analyzed with SPSS (version 23.0; SPSS, Inc., Chicago, IL, USA). All in vitro data were analyzed by one-way ANOVA. Statistical differences among groups were further analyzed using Tukey's post hoc test. The variables were compared between 26CO groups and 26NS groups using a Student's unpaired t-test. In all of the analyses, differences were considered statistically significant at p-value < 0.05.

5. Results

5.1. The RGNS treatment alleviated C2-ceramide-induced growth arrest and cellular senescence in C2C12 myoblasts

Cellular toxicities of RGNS, RGS and RG were examined in naïve (normal) and C-ceramide-treated C2C12 myoblasts. RGNS and RG did not exhibit any noticeable toxicity up to the concentration of 1000 μg/ml whereas RGS exhibited significant toxicity at over 500 μg/ml in both culture conditions (Fig. 2A and B). The treatment of C2-ceramide exerted a significant cellular toxicity of about 20% compared with the vehicle (DMSO)-treated control. Because the mass ratio of RGNS to RGS in RG extract was about 9:1, the in vitro test for comparing the efficacy of RGNS, RGS and RG was always executed at the ratio of 9:1:10. The protective effect of RGNS against C2-ceramide-induced cellular senescence was also confirmed using the BrdU cell proliferation assay (Fig. 2C). In order to cause senescence phenotypes such as the arrests of cell cycle and proliferation, and lysosomal dysfunction, C2-ceramide was added to the myoblasts and its intracellular accumulation was examined by staining with Oil Red O (Fig. 3A). After the treatment with C2-ceramide, the cytoplasm of C2C12 myoblast was also stained pale blue by β-galactosidase staining solution (Fig. 3A-b'), which indicates the cells enter the state of cellular senescence (permanent cell cycle arrest) [23]. In this condition of cellular senescence, the antisenescence effect of RGNS was compared with that of RGS. In the trypan blue exclusion assay, RGNS exhibited a dose-dependent protective effect against C2-ceramid-induced senescence and cell death and this protective effect was maintained for further 72 h (Fig. 3B). There was a significant increase of total cell number of RGNS- and C2-ceramide-treated C2C12 cells in a dose-dependent manner despite dead cell number was not increased in the same cultivation period. Protective effect of RGNS was more pronounced at 72 h after the treatment. In contrast, RGS or RG did not exhibit those protective effects. The protective effect of RGNS against C2-ceramide-induced cellular senescence was also confirmed in the β-galactosidase staining assay (Fig. 3C). The protective effect of RGNS against secretion of lysosomal β-galactosidase was significant in a dose-dependent manner. However, these effects were not observed with the treatments of RGS (data not shown).

5.2. The RGNS treatment restored C2-ceramide-induced mRNA expression of p57, atrogin-1, MuRF-1 and pax7 in C2C12 myoblasts

At the molecular level, the inhibitory effect of RGNS on the senescence-associated growth (cell cycle) arrest, autophagic proteolysis, and reduced ability to self-renew were evaluated in C2-ceramide-treated C2C12 myoblasts. The mRNA expression levels of cell cycle inhibitors such as p21 and p57, muscle-specific E3
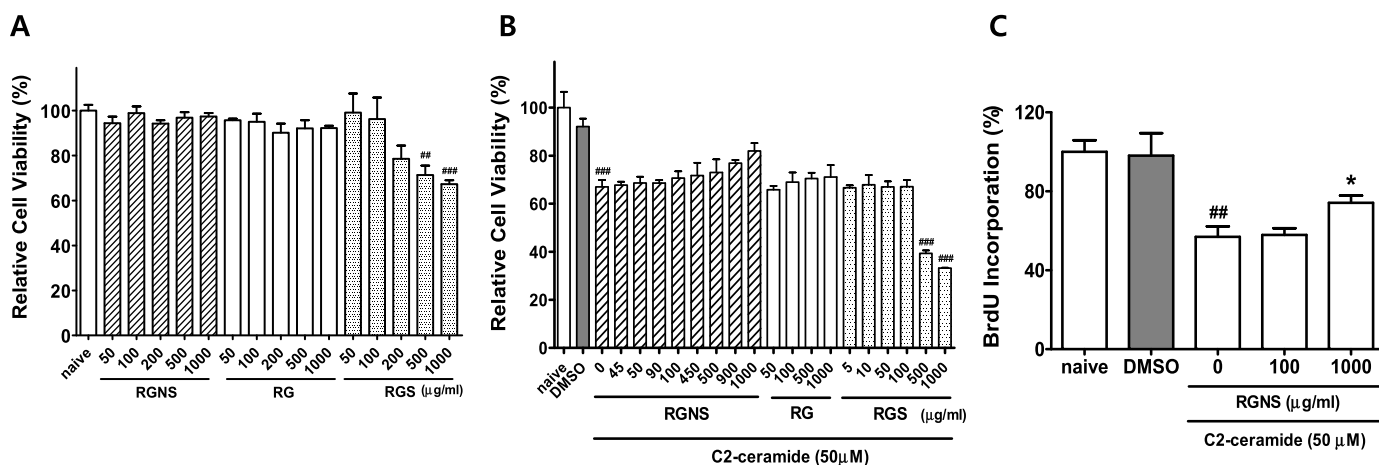
Fig. 2. Relative viabilities of naïve (A) and C2-ceramide-treated (B) C2C12 myoblasts assessed by EZ-Cytox® cell viability assay, and cell proliferation of the C2-ceramide-treated C2C12 myoblasts using BrdU labeling assay (C) after the treatments of RGNS, RG and RGS for 9 h. C2-Ceramide was dissolved in 100% DMSO. RGNS: non-saponin fraction of red ginseng; RGS: saponin fraction of red ginseng; RG: boiled water extract of red ginseng; DMSO: dimethyl sulfoxide. Data are presented as the mean ± SEM from at least three independent experiments. ##$p < 0.005$ and ###$p < 0.001$ vs. vehicle-treated C2C12 myoblasts (naïve in A, DMSO in B and C); *$p < 0.01$ vs. RGNS non-treated & C2-ceramid-treated C2C12 myoblasts.
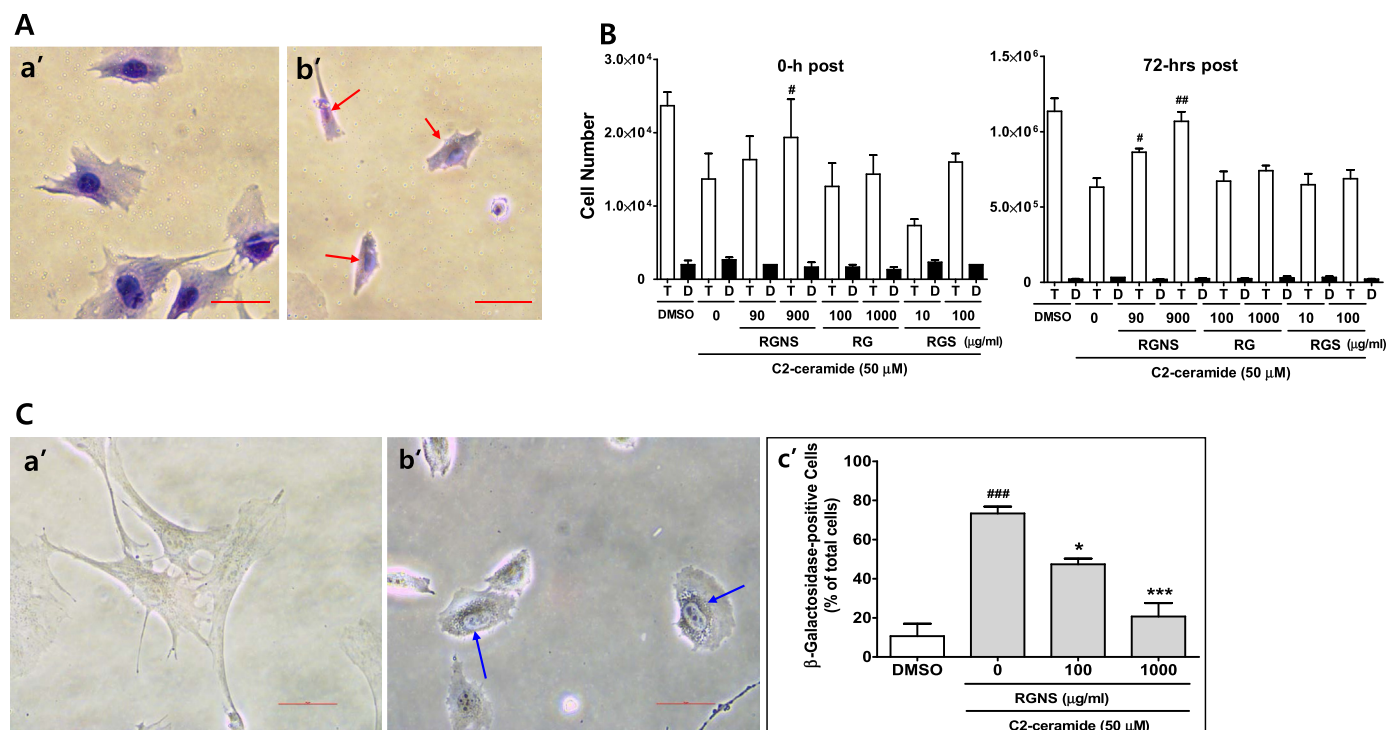
Fig. 3. Digital images of Oil red O-stained (naïve: A(a') and C2-ceramide-treated: A(b')), and β-galactosidase-stained C2C12 myoblasts (naïve: C(a'), C2-ceramide-treated: C(b'), the bar graph showing the RG(N)S effect on β-galactosidase-positive cell number: C(c')), and trypan blue exclusion assay (B) of C2C12 myoblasts immediately (0-hrs post) and 72 h (72-hrs post) after RG(N)S treatment. T: total cells (blue-stained and non-stained), D: dead cells (non-stained). RGNS: non-saponin fraction of red ginseng; RGS: saponin fraction; RG: water extract of red ginseng; DMSO: dimethyl sulfoxide. Red arrows in A(b') and blue arrows in C(b') indicate Oil red O-stained lipids (pinkish red), and the X-gal stain (blue) in the cytoplasm, respectively. Scale bar = 100 μm. Data are presented as the mean ± SEM from at least three independent experiments. $^{\#}p < 0.01$ and $^{\#\#}p < 0.005$ vs. C2-ceramide-treated C2C12 myoblast (DMSO); $^{*}p < 0.01$ and $^{***}p < 0.001$ vs. RGNS-non-treated & C2-ceramid-treated C2C12 myoblasts.

ubiquitin ligases such as atrogin-1 and MuRF-1, and pax7, a universal marker of myosatellite cells was analyzed by using RT-PCR (Fig. 4). Because cell cycle inhibitors negatively regulate the progression of cell cycle leading to blockage or reduction of cell proliferation, their increased expression is necessarily detected in senescence phase of the cells. In the present study, the mRNA expression of p57 was slightly increased by the C2-ceramide treatment and this increase is significantly inhibited by the 1000 μg/ml RGNS treatment below the basal level (Fig. 4E). However, the expression of p21 transcript did not affected by either C2-ceramide or RGNS. The C2-ceramide treatment significantly stimulated the mRNA expression of atrogin-1 and pax7, not MuRF-1 (Fig. 4A, B and C). And these increased expressions of atrogin-1 and pax7 transcripts were restored by the RGNS treatment in a dose-dependent manner although the statistical significance was not observed in pax7. In the case of atrogin-1, C2-ceramide induced 2.5-fold increase of the atrogin-1 mRNA expression, and this induction was completely inhibited by the treatments of 100 μg/ml and 1000 μg/ml RGNS (Fig. 4A).

### 5.3. Long-term administration of RGNS alleviated sarcopenic loss of hindlimb muscles in aged mice

In order to examine the effect of RGNS on skeletal muscle function regarding muscle strength and condition, the grip strength and hanging wire tests were performed at 1-week intervals during the feeding with RGNS-containing diet for 4 months. The RGNS diet significantly increased the grip strengths of 26-month-old mice (26NS) compared with those of vehicle-treated aged mice (26CO) fed the standard diet during the same period (Fig. 5A). The improvement of grip strength was most pronounced in the second

half of the RGNS-diet feeding period. In the hanging wire test, the strength improvement was also observed at third and fourth months in the RGNS-containing diet group (26NS) although not statistically significant on the last month (Fig. 5B). There were no significant differences in body weight and food consumption between 26CO and 26NS groups during the 4-month-feeding period (Fig. 5C and D).

Anti-senescence effect of RGNS was verified in the mouse model of sarcopenia. After 22-month-old mice were fed the reformulated diet containing 0.08% RGNS fraction (800 mg RGNS/kg-chaw) for 4 months, the weight alterations of their skeletal muscles such as TA, EDL, GN and SOL during the 4 month-feeding period were measured and compared with those of vehicle-treated mice. After feeding 22-month-old mice with standard chaw diet for 4 months, the weights of TA, EDL, GN and SOL muscles were decreased by 19.3, 23.2, 13.6 and 24.1%, respectively. These aging-associated decreases of muscle mass for 4 months were considerably restored by feeding of the RGNS diet although the restoration was statistically significant only in EDL and SOL muscles (Fig. 5).

5.4. Long-term administration of RGNS prevented the aging-associated reduction of cross-sectional area and fast-to-slow shift of muscle fiber type

Histopathological examinations of H&E-stained SOL muscle sections of 26-month-old mice (26CO) showed a significant decrease in CSAs of myofibers compared with those of 22-month-old mice (22CO) (Fig. 6A). Average sizes of CSAs in the 26CO group were decreased by almost 40%. This aging-associated reduction of CSA was significantly alleviated to 12.5% by feeding of RGNS diet for 4 months (Fig. 6B). The distribution of myofiber CSAs in SOL
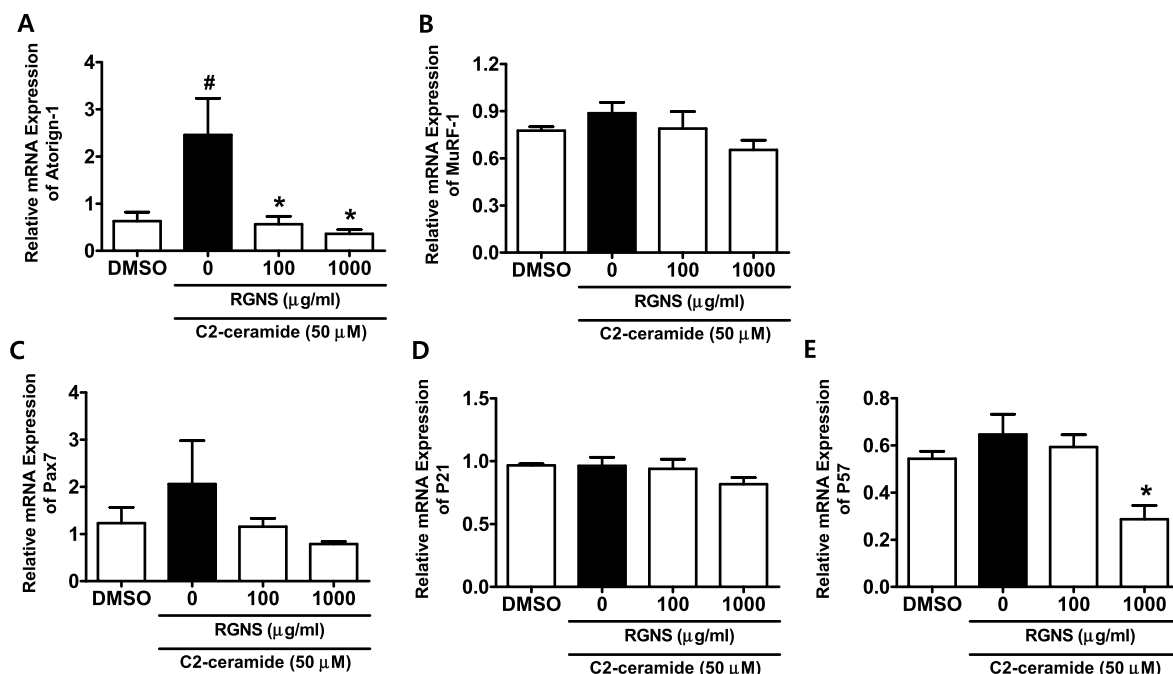
Fig. 4. Inhibitory effect of RGNS on mRNA expression levels of muscle-specific E3 ubiquitin ligases such as atrogin-1 (A) and MuRF-1 (B), cell cycle regulators such as p21 (C) and p57 (D), and pax7 (E), a universal skeletal muscle stem cell marker, in C2-ceramide-treated C2C12 myoblasts. RGNS: non-saponin fraction of red ginseng; DMSO: dimethyl sulfoxide. #$p < 0.01$ vs. vehicle-treated C2C12 myoblasts (DMSO); *$p < 0.01$ vs. C2-ceramide-treated C2C12 myoblasts.
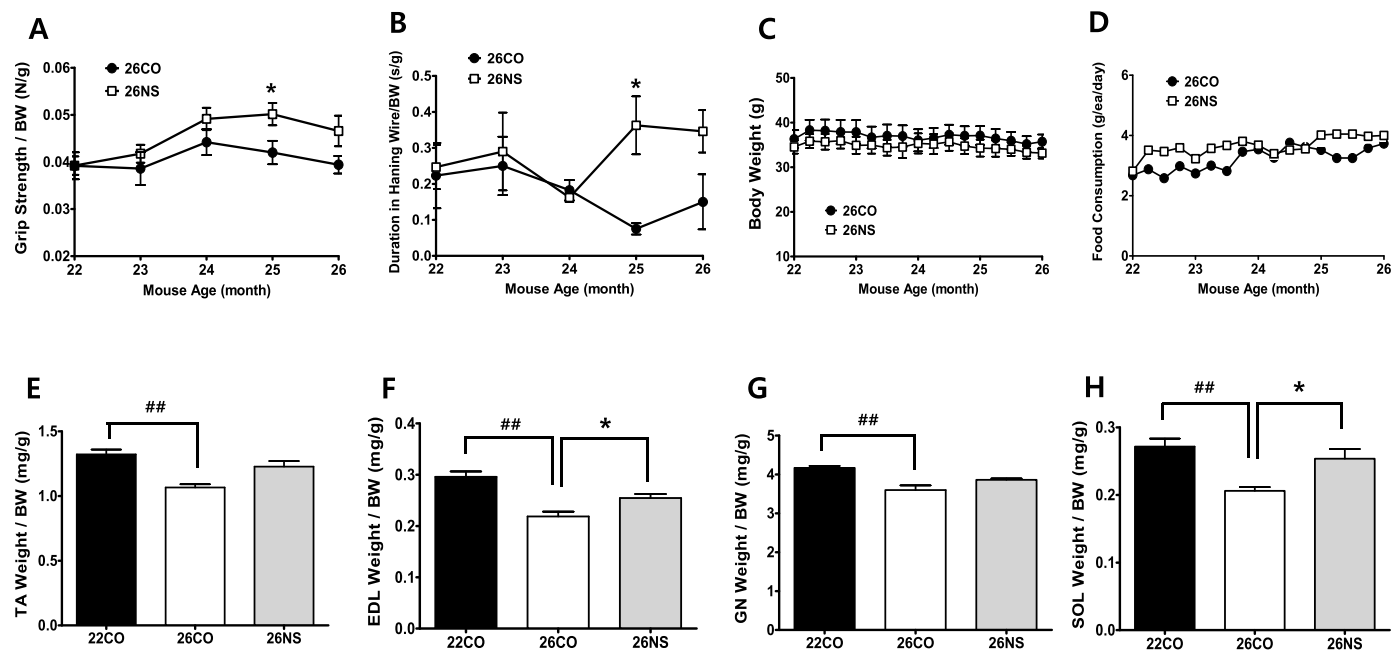
Fig. 5. Time-response curves of hindlimb grip strength (A), the duration in hanging wire test (B), body weights (C) and food consumption (D), and the muscle weights of tibialis anterior (E), extensor digitorum longus (F), gastrocnemius (G) and soleus (H) after 4-month-feeding of RGNS in aged mice. ##$p < 0.005$ vs. 22CO; *$p < 0.005$ vs. 26CO.

muscles also showed significant changes to smaller CSAs for 4 months, which was noticeably delayed by RGNS diet (Fig. 6C). The bell-shaped distribution curve ranging from 25 to 70 μm^2 CSAs with a peak of 40 μm^2 in 22CO group (blue line in C-d') was moved to the left ranging from 5 to 45 μm^2 with a peak of 30 μm^2 in 26CO group. And long-term feeding of RGNS diet recovered this aging-associated shift by half degree, as indicated in green line. We subsequently examined the aging-associated alterations of muscle

fiber type composition in SOL muscle by immunofluorescent staining of myosin heavy chains (MHCs) (Fig. 6D). The hindlimb skeletal muscles of rodents consist of four pure muscle fiber types (isomers): one slow myosin isoform MHC I, three fast isoforms such as MHC IIa, IId (IIx), and IIb, and several hybrid types such as I/IIa, IIa/IId and IId/IIb. Sarcopenia is characterized by the MHC shift of fast (type II)-to-slow (type I) twitch muscle fibers as well as the CSA reduction of muscle fibers [3]. After raising for 4 further months,
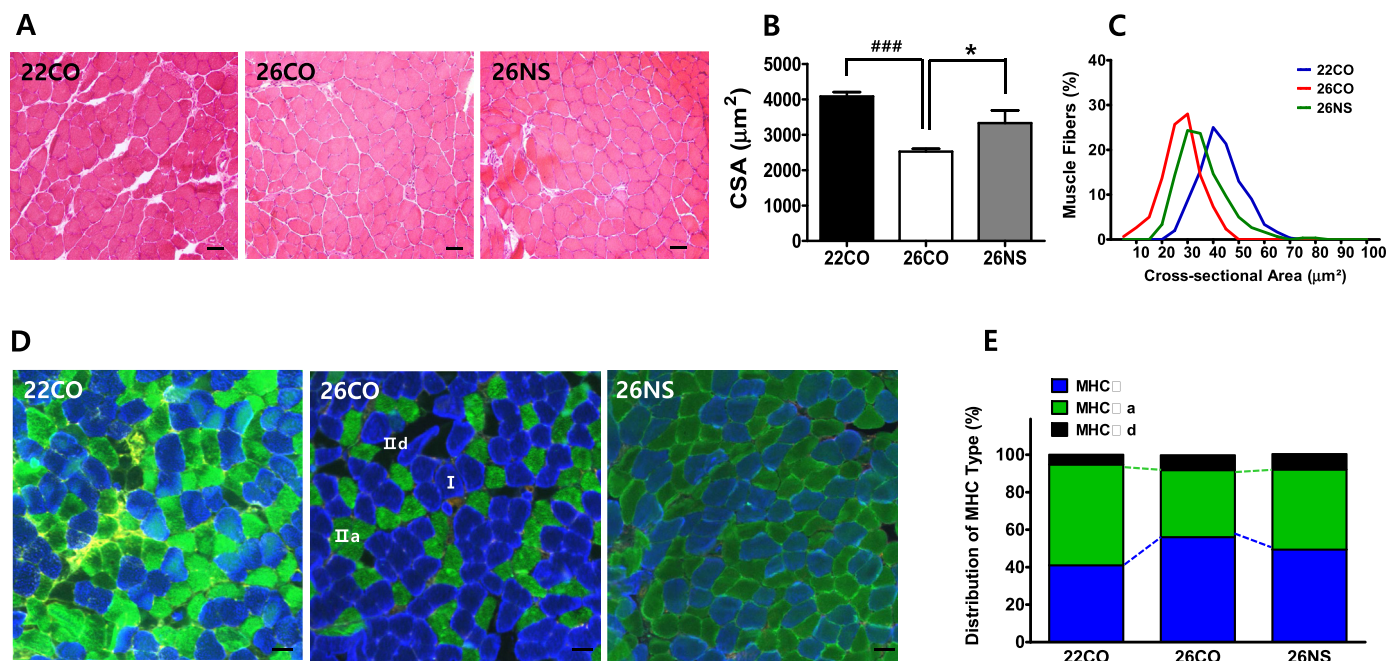
Fig. 6. H&E-stained (A) and MHC type-stained (D) images of the soleus muscle sections, and the graphs showing average cross-sectional area (B) and the distribution of CSA (C) and MHC type I, IIa and IId (E) in each group of the aged mice. Scale bar = 100 μm. Scale bar = 100 μm. Data are presented as the mean ± SEM from at least three independent samples. [###]p < 0.001 vs. 22CO; *p < 0.01 vs. 26CO.

the proportion of MHC I-type muscles in 26CO group has increased as much as the proportion of MHC IIa-type muscles has decreased (Fig. 6E). In the present study, the black-colored muscle fibers, unstained with MHC I and IIa, were considered MHC IId (IIx) because MHC IIb muscle fibers are not detected in the mouse soleus muscles [24]. The proportion of MHC IId were not changed significantly. This shift of fast-to-slow twitch fibers was restored by RGNS diet in 26NS group. In summary, it was observed that the long-term administration of RGNS-containing diet significantly alleviated an aging-associated decrease of SOL muscle mass indicated by H&E−stained images of SOL muscle sections (A), cross-sectional areas (CSAs) of the myofibers (B), the myofiber numbers of over 100 μm^2 CSA, and the MHC shift of fast-to-slow twitch fibers.

6. Discussion

Korean Red Ginseng which is widely known to have a powerful effect on immune-boosting and muscular enhancement, must be a good drug candidate. The current research aims non-saponin fraction of red ginseng (RGNS), a by-product generated by the extraction and fractionation of saponins in Korean Red Ginseng. Therefore, as long as its medical value is demonstrated, RGNS can secure both economic feasibility and medicinal effectiveness for resolving sarcopenia. In the present study, it was observed that the cellular toxicity of non-saponin fraction was significantly lower than that of saponin fraction when treated with equal mass, and non-saponin fraction produces nine times more than saponin fraction of the boiled water-extract of RG.

In order to study the mechanism of action of RGNS on muscle wasting and myogenesis in the C2C12 myoblasts, senescence (aging) was elicited by treating the cells with C2-ceramide. Cellular senescence is the result of gradual accumulation of a variety of cellular damages at molecular level, activating the expression of several pro-inflammatory genes. In the 1960s, Hayflick and Moorehead described the term "cellular senescence" as a permanent state of cell growth inhibition. Some aged cells secrete

inflammatory cytokines, chemokines, proteases, and senescence-associated secretory phenotypes (SASP), and senescence biomarkers include p21, a cyclin-dependent kinase inhibitor, and p27, a key regulator of cell proliferation [25−27].

When the cell entered the senescence phase, sphingomyelinases to generate ceramide through the hydrolysis of membrane sphingomyelin are activated, and thus intracellular level of ceramide considerably increased by about 4 folds [28,29]. Conversely, ceramide from the outside is able to cause a senescence phenotype in cells. When cells age, they lose their ability to divide and exhibit growth arrest with the up-regulation of cell cycle inhibitors such as p21 and p57, and the down-regulation of intracellular protein degradation mediated by E3 ubiquitin-protein ligase such as atrogin-1 and MuRF-1 [30−32]. In the present study, the transcript of atrogin-1 was conversely increased by C2-ceramide that was added to elicit cellular senescence, and this increase was significantly restored by the RGNS treatment. C2-Ceramide seems to act as a stressor to evoke intracellular proteolytic systems such as ubiquitin-proteasome system for maintaining cellular homeostasis as well as an aging trigger. In this respect, RGNS can also be considered an anti-stress agent that relieves the cellular stress caused by external stressor such as ceramide exposure. In the cellular level, the expressions of atrogin-1 and MuRF-1 transcripts are independently regulated through the activation of the P38 mitogen-active protein kinase and the nuclear factor Kappa B, respectively. Therefore, atrogin-1 can be expressed in a different pattern from MuRF-1 [32]. Along with the autophagy-lyosome machinery, ubiquitin-proteasome system is the most important cell proteolytic system that control protein turnover in muscle and maintain muscle homeostasis. In muscle atrophy, muscle-specific E3 ligases such as atrogin-1/MAFbx and MuRF1 are upregulated and thus these ligases can be used as biomarkers for the alteration of muscle mass in in vitro and in vivo models of muscle atrophy. Although protective role of RGNS against intracellular protein degradation has been investigated at molecular level, further studies are needed in terms of changes in the expression of

myogenesis-related genes or changes in intracellular protein synthesis.

P57 responded significantly to the RGNS treatment but p21 did not in the present study. Cell proliferation and differentiation in part can be regulated at the level of cell cycle by cyclin/cyclin-dependent kinase (CDK) complexes whose activities are negatively regulated through the interaction with CDK inhibitors (CKIs). Among the two families of CKIs, the CIP/KIP family includes p21Cip1 (p21), p27Kip1 (p27), and p57Kip2 (p57), and have known to play a critical role in the differentiation of certain cell types. p57 mainly inhibits the G1 phase during the repetitive senescence and the G2 phase during the premature senescence whereas p21 interferes with the expression of genes necessary for DNA synthesis in S phase of the cell cycle. P57 is a master regulator of the cell cycle in embryogenesis and tissue differentiation as well as the senescence induction upon cellular stress, which is not shared by the other members of the CIP/KIP family such as p21 and p27, and their expression can be differentially controlled under the conditions of quiescence or senescence [33,34]. Therefore, this result implies that RGNS can exert a wide range of defensive roles against cellular stress from the outside.

In the present study, we used 22-month-old female mouse as an experimental in vivo model of sarcopenia although it is known that males with fewer factors affecting muscle performance, such as menstruation, are more suitable for muscle research than females. In order to minimize the effect of femaleness, the changes of mouse body weight were inspected for entire period of the experiment, and all muscle weight data were calibrated based on body weight on sampling time point. During the 4-month-experimental period, the weights of 22-month-old mice remained almost unchanged, and even during each month, regardless of the menstrual cycle, as shown in Fig. 5C. The improvement in muscle performance indicated by grip strength and the duration in hanging wire tests was more evident in the second two months of the total 4-month RGNS administration period, and in the case of grip strength, the improvement gradually increased as the administration period increased, and the highest at the end of the administration (Fig. 5A). This means that long-term administration is needed to achieve the therapeutic effect of RGNS-containing diet on sarcopenia.

The soleus muscle is mainly composed of fast-twitch muscle fibers (MHC II) in the rodents, ranging from 64 to 100%, and as aging progresses, a shift from fast-to slow-twitch muscle proceeds in a continuity of 'MHC IIb ↔ IIb/IId ↔ IId ↔ IIa/IId ↔ IIa ↔ I/IIa ↔ I' with hybrid fibers being intermediate to pure fibers [7,23,35]. In the SOL muscle of 22-month-old mouse (22CO), the proportion of fast-twitch muscle (MHC I) was about 60% that is lower than that (60%) of fast-twitch muscle (MHC IIa). This might be due to the fact that the significant portion of MHC IIa seems to be the increase of hybrid types like MHC I/IIa, and the most hybrid fibers are composed of IIC type (IIa > I), which is apparently close to IIa. This ratio of fast-to slow-twitch muscle in SOL muscle in the 22CO group was reversed by raising 4 further months. Interestingly, the 4-month-feeding of RGNS significantly restored the aging-associated shift of fast-to slow-twitch muscles in SOL muscle, which is precisely coincident with the results of RGNS-elicited restoration of hindlimb muscle weights and their CSAs in the 26-minth-old mice. It is noticeable that although a long-term period is required, the present results that daily consumption of RGNS through daily diet can improve physical and physiological functions of atrophied muscles in the aged mice provide groundbreaking potential for treating sarcopenia.

Declaration of competing interest

The authors declare that they have no conflicts of interest.

Acknowledgement

References

[1] Choi KM. Sarcopenia and sarcopenic obesity. Korean J Intern Med 2016;31: 1054–60.
[2] Morley JE, Malmstrom TK, Rodriguez-Manas L, Sinclair AJ. Frailty, sarcopenia and diabetes. J Am Med Dir Assoc 2014;15:853–9.
[3] Miljikovic N, Lim JY, Iva M, Frontera WR. Aging of skeletal muscle fibers. Ann Rehabil Med 2015;39:155–62.
[4] Lee M, Oilkawa S, Ushida T, Suzuki K, Akimoto T. Effects of exercise training on growth and differentiation factor 11 expression in aged mice. Front Physiol 2019;10:970.
[5] Cruz-Jentoft AJ, Baeyens JP, Bauer JM, Boirie Y, Cederholm T, Landi F, Martin FC, Michel JP, Rolland Y, Schneider SM, et al. Sarcopenia: European consensus on definition and diagnosis: report of the European working group on sarcopenia in older people. Age Ageing 2010;39:412–23.
[6] Woo J. Sarcopenia. Clin Geriatr Med 2017;33:305–14.
[7] White ZR. Protein homeostasis and sarcopenia: the influence of fasting and exercise on protein synthesis and degradation pathways [dissertation]. Crawley (WA): University of Western Australia; 2016.
[8] Brook MS, Wilkinson DJ, Phillips BE, Perez-schindler J, Phip A, Smith K, Atherton PJ. Skeletal muscle homeostasis and plasticity in youth and ageing: impact of nutrition and exercise. Acta Physiol 2016;216:15–41.
[9] Enwere EK, Lacasse EC, Adam NJ, Korneluk RG. Role of the TWEAK-Fn14-cIAP1-NF-κB signaling axis in the regulation of myogenesis and muscle homeostasis. Front Immunol 2014;5:34.
[10] Wen Y, Bi P, Liu W, Asakura A, Keller C, Kuang S. Constitutive Notch activation upregulates PAX7 and promotes the self-renewal of skeletal muscle satellite cells. Mol Cell Biol 2012;32:2300–11.
[11] Sharples AP, Al-Shanti N, Lewis MP, Stewart CE. Reduction of myoblast differentiation following multiple population doublings in mouse C2C12 cells: a model to investigate ageing. J Cell Biochem 2011;112:3773–85.
[12] Kwak JY, Kwon KS. Pharmacological interventions for treatment of sarcopenia: current status of drug development for sarcopenia. Ann Geriatr Med Res 2019;23:98–104.
[13] Jang DJ, Lee MS, Shin BC, Lee YC, Ernst E. Red ginseng for treating erectile dysfunction: a systematic review. Br J Clin Pharmacol 2008;66:444–50.
[14] Lee SM, Bae BS, Park HW, Ahn NG, Cho BG, Cho YL, Kwak YS. Characterization of Korean red ginseng (Panax ginseng Meyer): history, preparation method, and chemical composition. J Ginseng Res 2015;39:384–91.
[15] Kim YH, Park HR, Cha SY, Lee SH, Jo JW, Go JN, Lee KH, Lee SY, Shin SS. Effect of red ginseng natural GEL on skin aging. J Ginseng Res 2020;44:115–22.
[16] Dong Z, Xu M, Huang J, Chen L, Xia J, Chen X, Jiang R, Wang L, Wang Y. The protective effect of ginsenoside Rg1 on aging mouse pancreas damage induced by D-galactose. Exp Ther Med 2017;14:616–22.
[17] Hou J, Yun Y, Xue J, Jeo B, Kim S. Doxorubicin-induced normal breast epithelial cellular aging and its related breast cancer growth through mitochondrial autophagy and oxidative stress mitigated by ginsenoside Rh2. Phytother Res 2020;34:1659–69.
[18] Zeng Y, Hu W, Jing P, Chen X, Wang Z, Wang L, Wang Y. The regulation of ginsenoside Rg1 upon aging of bone marrow stromal cell contribute to delaying senescence of bone marrow mononuclear cells (BMNCs). Life Sci 2018;209:63–8.
[19] Nam GY, Go SR, Choe GJ. Relationship of saponin and non-saponin for the quality of ginseng. J Ginseng Res 1998;22:274–83.
[20] Park YC, Lim JD, Kim JB, Lee S. Review of red ginseng in terms of mechanisms for pharmacodynamics and toxicity. J Korean Oriental Med 2012;33(3): 200–30.
[21] Jadhav KS, Dungan CM, Williamson DL. Metformin limits ceramide-induced senescence in C2C12 myoblast. Mech Ageing Dev 2013;34:548–59.
[22] Zhu XF, Liu ZC, Xie BF, Feng GK, Zeng YX. Ceramide induces cell cycle arrest and upregulates p27kip in nasopharyngeal carcinoma cells. Cancer Lett 2003;193:149–54.
[23] Dimri GP, Lee X, Basile G, Acosta M, Scott G, Roskelley C, Medrano EE, Linskens M, Rubelj I, Pereira-Smith O, Peacocke M, Campisi J. A biomarker that identifies senescent human cells in culture and in aging skin in vivo. Proc Natl Acad Sci USA 1995;92:9363–7.
[24] Augusto V, Padovani CR, Campos GER. Skeletal muscle fiber types in C57BL/6J mice. Braz J Morphol Sci 2004;21:89–94.
[25] LeBrasseur NK, Tchkonia T, Kirkland JL. Cellular senescence and the biology of aging, disease, and frailty. Nestle Nutr Inst Workshop Ser 2015;83:11–8.
[26] Rossi MN, Antonangeli F. Cellular response upon stress: p57 contribution to the final outcome. Mediat Inflamm 2015;2015:259325.
[27] Lopes-Paciencia S, Saint-Germain E, Rowell M-C, Ruiz AF, Kalegari P, Ferbeyre G. The senescence-associated secretory phenotype and its regulation. Cytokine 2019;117:15–22.
[28] Venable ME, Lee JY, Smyth MJ, Bielawska A, Obeid LM. Role of Ceramide in cellular senescence. J Biol Chem 1995;270:30701–8.

[29] Zhu S, Tian Z, Torigoe D, Zhao J, Xie P, Sugizaki T, Sato M, Horiguchi H, Terada K, Dadomatsu T, et al. Aging- and obesity-related peri-muscular adipose tissue accelerates muscle atrophy. PLoS One 2019;14:e0221366.

[30] Gumucio JP, Mendias CL. Atrogin-1, MuRF-1, and sarcopenia. Endocrine 2013;43:12–21.

[31] Deursen JM. The role of senescence cells in ageing. Nature 2014;509:439–46.

[32] Natanek SA, Riddoch-Contreras J, Marsh GS, Hopkinson NS, Moxham J, Man WD, Kemp PR, Polkey MI. MuRF-1 and atrogin-1 protein expression and quadriceps fiber size and muscle mass in stable patients with COPD. COPD 2013;10:618–24.

[33] Rossi MN, Antonangeli F. Cellular response upon stress: p57 contribution to the final outcome. Mediat Inflamm 2015;2015:259325.

[34] Shankland SJ, Eitner F, Hudkins KL, Goodpaster T, D'Agati V, Alpers CE. Differential expression of cyclin-dependent kinase inhibitors in human glomerular disease: role in podocyte proliferation and maturation. Kidney Int 2000;58:674–83.

[35] Claflin DR, Larkin LM, Cederna PS, Horowitz JF, Alexander NB, Cole NM, Galecki AT, Chen S, Nyquist LV, Carlson BM, et al. Effects of high- and low-velocity resistance training on the contractile properties of skeletal muscle fibers from young and older humans. J Appl Physiol 1985;111(2011): 1021–30.